Journal of Applied Fluid Mechanics, Vol. 9, No. 4, pp. 2097-2103, 2016.
Available online at www.jafmonline.net, ISSN 1735-3572, EISSN 1735-3645.
DOI: 10.18869/acadpub.jafm.68.235.19346

Radiation and Viscous Dissipation Effects on Laminar Boundary Layer Flow Nanofluid over a Vertical Plate with a Convective Surface Boundary Condition with Suction

K. Gangadhar

Department of Mathematics, ANUOC, Ongole-523001, A. P, India.

Email: kgangadharmaths@gmail.com

(Received October 1, 2011; accepted October 18, 2015)

ABSTRACT

The problem of laminar radiation and viscous dissipation effects on laminar boundary layer flow over a vertical plate with a convective surface boundary condition is studied using different types of nanoparticles. The general governing partial differential equations are transformed into a set of two nonlinear ordinary differential equations using unique similarity transformation. Numerical solutions of the similarity equations are obtained using the Nachtsheim-Swigert Shooting iteration technique along with the fourth order Runga Kutta method. Two different types of nanoparticles copper water nanofluid and alumina water nanofluid are studied. The effects of radiation and viscous dissipation on the heat transfer characteristics are discussed in detail. It is observed that as Radiation parameter increases, temperature decreases for copper water and alumina water nanofluid and the heat transfer coefficient of nanofluids increases with the increase of convective heat transfer parameter for copper water and alumina water nanofluids.

Key words: Laminar boundary layer; Nanofluids; Radiation; Viscous dissipation.

NOMENCLATURE

$Bi = \frac{h}{k}\sqrt{\frac{\nu_{nf}}{U_\infty}}$ convective heat transfer parameter

$(Ec)_{nf} = \frac{\mu_{nf} U_\infty^{\,2}}{(\rho c_p)_{nf}\, \nu_{nf}\, (T_w - T_\infty)}$ Eckert number

k_{nf} effective thermal conductivity of the nanofluid

$(\rho C_p)_{nf}$ heat capacity of the nanofluid

$(\mathrm{Pr})_{nf} = \nu_{nf} / \alpha_{nf}$ Prandlt number

$Nr = \frac{16\sigma^* T_\infty^3}{3k_{nf}\, k^*}$ radiation parameter.

$f_w = \frac{2x^{1/2}}{U_\infty \nu_{nf}} v_w > 0$ suction parameter

k_f thermal conductivity of the fluid

k_s thermal conductivity of the solid

H heat transfer coefficient

K thermal conductivity coefficient

q_r radiative heat flux

T temperature of the nanofluid

Greek Symbols

α_{nf} thermal diffusivity of the nanofluid

ρ_{nf} effective density of the nanofluid

μ_f viscosity of the fluid

ρ_f reference density of the fluid fraction

ρ_s reference velocity of the solid fraction

μ_f viscosity of the fluid fraction

μ_{nf} effective viscosity of the nanofluid

φ solid volume fraction of the nanofluid

1. INTRODUCTION:

As diverse industrials including microelectronics, transportation, and manufacturing become more advanced, cooling technology is one of the most important challenges Go *et al*. (2001). Some works were done on the effects of nanofluids on forced convection heat transfer. Maiga *et al*. (2004) studied numerically forced convection of Al_2O_3-water and Al_2O_3-ethylene glycol nanofluids in a straight tube of circular cross-section using the single phase

model. They considered both laminar and turbulence flows. Their results for laminar flow showed increase in rate of heat transfer and skin friction coefficient with increasing volume fraction of the nanoparticles. For turbulent flow they observed that the heat transfer coefficient increases steeply for a very short distance from the inlet section. Moreover they found that the Al_2O_3-ethylene glycol nanofluid is more effective than to the Al_2O_3-water nanofluid in heat transfer enhancement.

Recently, Sheikhzadeh *et al*. (2011) conducted that a numerical simulation to investigate the problem of free convection of the TiO_2-water nanofluid in rectangular cavities differentially heated on adjacent walls. The left and the top walls of the cavities were heated and cooled; respectively, while; the cavities right and bottom walls were kept insulated. They found that by increase in the volume fraction of the nanoparticles, the mean Nusselt number of the hot wall increases for the shallow cavities; while, the reverse trend occurs for the tall cavities. Witharana *et al*. (2011) analyzed the Stability of nanofluids in quiescent and shear flow fields. Yacob *et al*. (2011) was analysed the Boundary layer flow past a stretching/shrinking surface beneath an external uniform shear flow with a convective surface boundary condition in a nanofluid. Hamad and Pop. (2011) have discussed the Unsteady MHD free convection flow past a vertical permeable flat plate in a rotating frame of reference with constant heat source in a nanofluid. Emmanuel *et al*. (2011) discussed the investigations on the nanolayer heat transfer in nanoparticles- in-liquid suspensions. Anjali Devi and Julie Andrews (2011) investigated the laminar boundary layer flow of nanofluid over a flat plate. Tahery *et al*. (2010) discussed the Numerical Study of Heat Transfer Performance of Homogenous Nanofluids under Natural Convection. Tania S. Khaleque and Samad (2010) discussed the Effects of Radiation, Heat Generation and Viscous Dissipation on MHD Free Convection Flow along a Stretching Sheet

All the above mentioned papers did not study the combined effects of convective boundary condition and suction; hence the present paper studied the laminar boundary layer flow over a vertical plate in a nanofluid with radiation and viscous dissipation effects in the presence of convective boundary condition and suction and results are presented in graphs showing the influence of the emerging parameters.

2. MATHEMATICAL ANALYSIS

It is considered a steady two-dimensional laminar boundary layer flow past a vertical plate in a water-based nanofluid containing different type of nanoparticles, namely, copper water nanofluid, and aluminium water nanofluid, with radiation effects are considered and the nanofluid is assumed incompressible and the flow is assumed to be laminar. The physical properties of the nanofluids are given in Table 1.

Further, we consider a Cartesian coordinate system (x, y), where x and y are the coordinates measured along the plate and normal to it, respectively, and the flow takes place at $y = 0$. It is also assumed that the temperature of the plate is $T_w(x)$ and that of the ambient nanofluid is T_∞ . Following Golia and Viviani (1985, 1986) and Magyari and Chamkha (2007) the surface tension σ is assumed to vary linearly with temperature as $\sigma = \sigma_0[1-\gamma(T-T_0)$ where σ_0 and T_0 are the surface tension and temperature at the slit, respectively and it is assumed that $T_0 \cong T_\infty$. For most liquids the surface tension σ decreases with temperature, i.e. γ is a positive fluid property.

The steady boundary layer equations for a nanofluid in the coordinates $\overline{x}$ and $\overline{y}$ are (see Christopher and Wang (2001) and Tiwari and Das (2007))

$$\frac{\partial u}{\partial x}+\frac{\partial v}{\partial y}=0 \tag{1}$$

$$u\frac{\partial u}{\partial x}+v\frac{\partial u}{\partial y}=\nu_{nf}\frac{\partial^2 u}{\partial y^2} \tag{2}$$

$$u\frac{\partial T}{\partial x}+v\frac{\partial T}{\partial y}=\frac{\alpha_{nf}}{\nu_{nf}}\frac{\partial^2 T}{\partial y^2}-\frac{1}{(\rho c_p)_{nf}}\frac{\partial q_r}{\partial y}+\frac{\mu_{nf}}{(\rho c_p)_{nf}}\left(\frac{\partial u}{\partial y}\right)^2 \tag{3}$$

Subject to the boundary conditions

$$\begin{aligned} &u(x,o)=v_w, v(x,0)=0, -k\frac{\partial T}{\partial y}=h\,(T-T_w(x,0)],\\ &u(x,\infty)=U_\infty, T(x,\infty)=T_\infty \end{aligned} \tag{4}$$

where u and v are velocity components along the x and y axes, respectively

$$\alpha_{nf}=\frac{k_{nf}}{(\rho C_p)_{nf}}$$

$$\rho_{nf}=(1-\varphi)\rho_f+\varphi\rho_s.$$

$$\mu_{nf}=\frac{\mu_f}{(1-\varphi)^{2.5}}$$

$$(\rho C_p)_{nf}=(1-\varphi)(\rho C_p)_f+\varphi(\rho C_p)_s$$

$$k_{nf}=k_f\left\{\frac{(k_s/k_f)+(n-1)-(n-1)\varphi(1-(k_s/k_f))}{(k_s/k_f)+(n-1)-\varphi(1-(k_s/k_f))}\right\}$$

Table 1 Physical properties of base fluid water, copper, aluminia at 20^0C(293K)

	$\rho(Kg/m^3)$	$C_p(J/Kg.K)$	$k(W/m.K)$
Water	1000.52	4181.8	0.597
Copper	8954	383.1	386
Alumina	3970	769	36

Using the Rosseland approximation for radiation (1992), the radiative heat flux is simplified as

Table 2 Thermal physical properties of copper water nanofluid

φ	ρ_{nf}	$(C_p)_{nf}$	μ_{nf}	k_{nf}	$(\mathrm{Pr})_{nf}$
0.00	1000.52	4181.80	0.001002	0.5970	7.02
0.01	1080.05	4143.81	0.001027	0.6554	6.06
0.02	1159.59	4105.82	0.001053	0.7150	5.30
0.03	1239.12	4067.83	0.001081	0.7758	4.68
0.04	1318.85	4029.85	0.001109	0.8379	4.17
0.05	1398.19	3991.86	0.001139	0.9012	3.75
0.06	1477.72	1477.72	3953.88	0.001169	3.39
0.07	1557.26	3915.89	0.001201	1.0321	3.09
0.08	1636.79	3877.90	0.001234	1.0996	2.83
0.09	1716.33	3839.91	0.001268	1.1687	2.60

$$q_r = -\frac{4}{3}\frac{\sigma^*}{k^*}\frac{\partial T^4}{\partial y} \tag{5}$$

Where σ* is the Stefan-Boltzmann constant and k^* is the mean absorption coefficient. It is assumed that the temperature differences within the flow such the term T^4 may be expressed as a linear function of temperature. This is accomplished by expanding T^4 in a Taylor's series about T_∞ and neglecting higher-order terms, thus

$$T^4 \cong 4T_\infty^3 T - 3T_\infty^4 \tag{6}$$

Using equations (4), (5) and (6), Eq. (3) reduces to

$$u\frac{\partial T}{\partial x} + v\frac{\partial T}{\partial y} = \frac{\alpha_{nf}}{\nu_{nf}}(1+Nr)\frac{\partial^2 T}{\partial y^2} + \frac{\mu_{nf}}{(\rho c_p)_{nf}}\left(\frac{\partial u}{\partial y}\right)^2 \tag{7}$$

Similarity solution of (2)-(4) subject to the boundary conditions (5) of the following form:

$$\psi(x,y) = (U_\infty \nu_{nf} x)^{1/2} f(\eta)$$
$$\eta = y\left(\frac{U_\infty}{\nu_{nf} x}\right)^{1/2}, \theta = \frac{T - T_\infty}{T_w - T_\infty} \tag{8}$$

Where $\psi(x,y)$ is the stream function which is defined as

$u = \frac{\partial \psi}{\partial y}, v = \frac{-\partial \psi}{\partial x}$ and θ is the dimension less temperature. In terms of these new variables, the velocity components can be expressed as

$$u = U_\infty f'(\eta)$$
$$v = \frac{1}{2}\left(\frac{\nu_{nf} U_\infty}{x}\right)^{1/2}(\eta f'(\eta) - f(\eta)) \tag{9}$$

The transformed momentum and energy equations together with the boundary conditions Equations (4), (2) and (7) can be written as

$$f''' + \frac{1}{2}ff'' = 0 \tag{10}$$

$$(1+Nr)\theta'' + \frac{1}{2}(\mathrm{Pr})_{nf} f\theta' + (\mathrm{Pr})_{nf}(Ec)_{nf} f''^2 = 0 \tag{11}$$

With boundary conditions

$$\eta = 0, y = 0, f = fw, f' = 0, \theta' = Bi[\theta - 1]$$
$$\eta \to \infty, y \to \infty, f' = 1, \theta = 0 \tag{12}$$

Where the prime denote differentiation with respect to η.

3. NUMERICAL ANALYSIS

In order to evaluate the numerical values of the density, viscosity, heat capacity, viscosity, density, thermal conductivity, kinematic viscosity and thermal diffusivity for copper water and alumina water nanofluid for different values of volume fraction, fortran program is used. The set of non-linear coupled differential Equations (10) and (11) subject to the boundary conditions (12) constitute a two-point boundary value problem. In order to solve these systems of transformed equations together with the boundary conditions, ordinary methods fail. Hence the equations (10) and (11) are solved numerically subject to boundary conditions using Nachtsheim-Swigert Shooting iteration technique and Runge-Kutta method. Initial guesses were made taking into account of convergency and numerical results were obtained for several values of the physical parameters Nr, Bi, $(\mathrm{Pr})_{nf}$, $(Ec)_{nf}$. The local heat transfer for nanofluids is given by

$$\theta'(0) \text{ and } \left(\frac{\partial \theta}{\partial \eta}\right)_{\eta=0} = 0.332(\mathrm{Pr})_{nf}^{1/3}$$

4. RESULTS AND DISCUSSION:

The heat transfer problem associated with laminar flow of the nanofluids over a vertical plate has been studied. Table 2 and Table 3 indicate the physical and thermal properties of copper water nanofluid. Table 4 depicts the different values of alumina water nanofluid.

Figure 1 and 2 shows the dimensionless velocity and temperature profile of the boundary layer for Copper-water nanofluid for different suction parameter. It is observed that as suction parameter

increases, velocity increases and temperature decreases.

Table 3 Thermal physical properties of copper water nanofluid

φ	$\nu_{nf} \times 10^6$	$\alpha_{nf} \times 10^6$
0.00	1.0014790	0.1426873
0.01	0.9513360	0.1569280
0.02	0.9088625	0.1715080
0.03	0.8726166	0.1864290
0.04	0.8455057	0.2017176
0.05	0.8146879	0.2173510
0.06	0.7915044	0.2334037
0.07	0.7714330	0.2498296
0.08	0.7540548	0.2666551
0.09	0.7390309	0.2839309
0.10	0.7260842	0.3059676

Table 4 Thermal physical properties of Alumina water nanofluid

φ	ρ_{nf}	$(C_p)_{nf}$	μ_{nf}	k_{nf}	$(Pr)_{nf}$
0.00	000.52	4181.80	0.001002	0.5970	7.02
0.01	031.22	4147.73	0.001027	0.6142	6.94
0.02	1059.91	4113.54	0.001053	0.6318	6.86
0.03	1089.60	4079.42	0.001081	0.6496	6.79
0.04	1119.30	4045.29	0.001109	0.6679	6.72
0.05	1148.99	4011.16	0.001139	0.6865	6.66
0.06	1178.69	3977.03	0.00116	0.7055	6.59
0.07	1208.38	3942.90	0.001201	0.7249	6.53
0.08	1238.08	3908.78	0.001234	0.7446	6.48
0.09	1267.77	3874.65	0.001268	0.7648	6.43

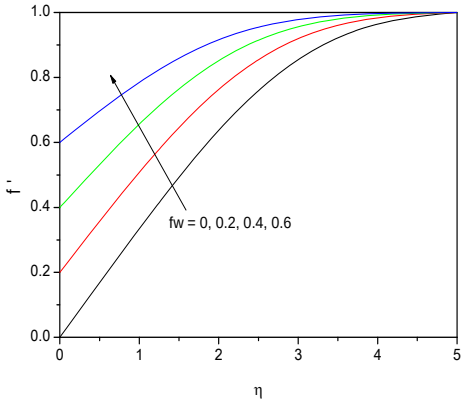

Fig. 1. Velocity profiles for copper water nanofluid with $\varphi = 0.1$, Bi=0.1& Ec=0.1 for various fw.

Figure 3 shows the dimensionless temperature profile of the boundary layer for Copper-water nanofluid for different Radiation parameter. It is observed that as Radiation parameter increases, temperature decreases. Physically, thermal radiation is electromagnetic radiation generated by the thermal motion of charged particles in matter Figure 4 and 5 displays the dimensionless temperature profile of the boundary layer for Copper-water nanofluid for different Eckert number and Convective heat transfer parameter. It is observed that as Eckert number and Convective heat transfer parameter increases, temperature increases. Fluid on adjacent layers due to the action of shear forces is transformed into heat is defined as viscous dissipation.

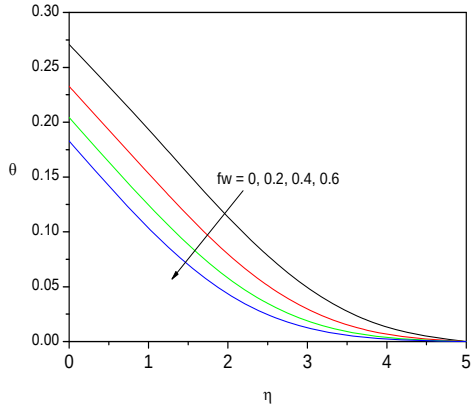

Fig. 2. Temperature profiles for copper water nanofluid with $\varphi = 0.1$, Bi=0.1& Ec=0.1 for various fw.

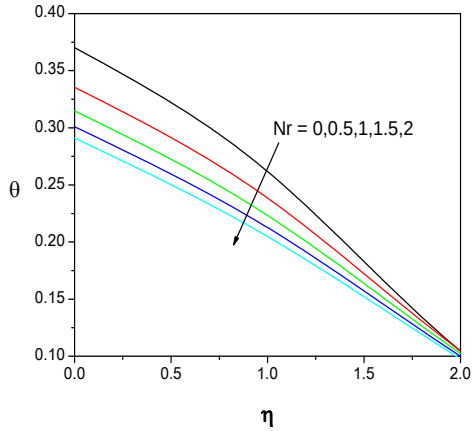

Fig. 3. Temperature profiles for copper water nanofluid with $\varphi = 0.1$, Bi=0.1& Ec=0.1 for various *Nr*.

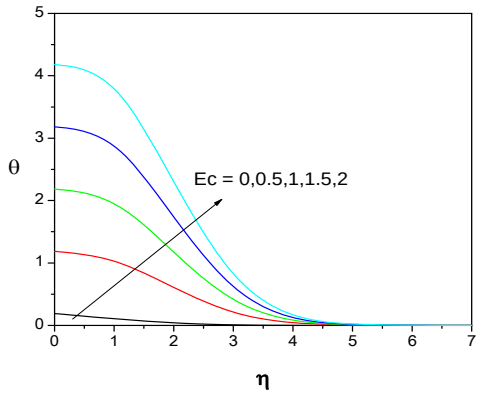

Fig. 4. Temperature profiles for Copper water nanofluid with Bi=0.1, $\varphi = 0.1$ and Nr=0.1 for various *Ec*.

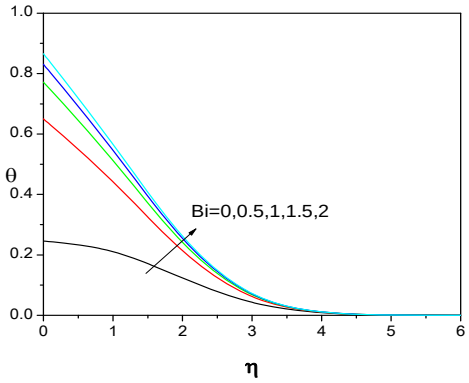

Fig. 5. Temperature profiles for Copper water nanofluid with Ec=0.1, $\varphi = 0.1$ & Nr=0.1 for various *Bi.*

Figure 6 shows the dimensionless temperature profile of the boundary layer for Copper-water nanofluid for different volume fraction. It is observed that as volume fraction increases, temperature decreases.

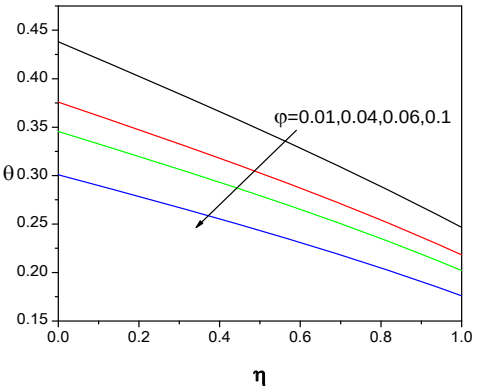

Fig. 6. Effect of volume fraction on temperature profile of copper water nanofluid.

Figure 7 shows the dimensionless temperature profile of the boundary layer for Alumina-water nanofluid for different Radiation parameter. It is observed that as Radiation parameter increases, temperature decreases.

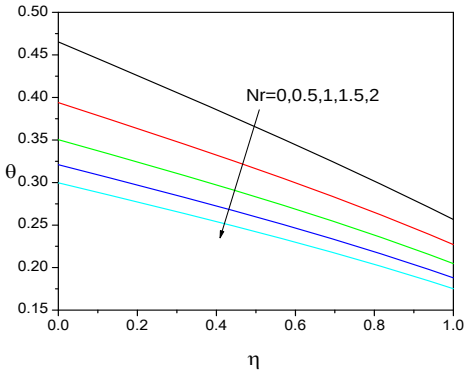

Fig. 7. Temperature profiles for Alumina water nanofluid with Bi=0.1, $\varphi = 0.1$ & Ec=0.1 for various *Nr*.

Figure 8 and 9 displays the dimensionless temperature profile of the boundary layer for Alumina-water nanofluid for different Eckert number and Convective heat transfer parameter. It is observed that as Eckert number and Convective heat transfer parameter increases, temperature increases.

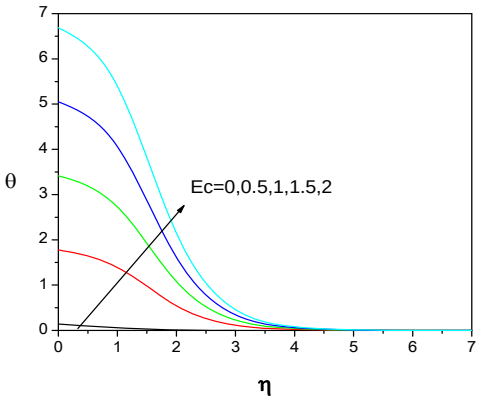

Fig. 8. Temperature profiles for Alumina water nanofluid with Bi=0.1, $\varphi = 0.1$ & Nr=0.1 for various *Ec.*

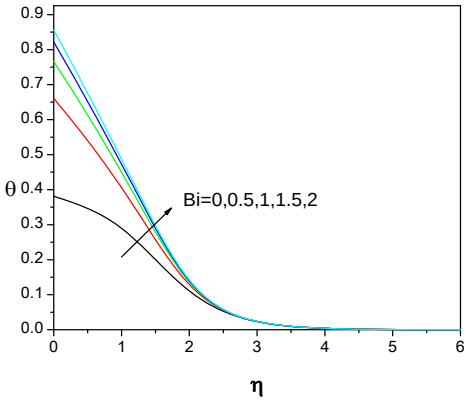

Fig. 9. Temperature profiles for Alumina water nanofluid with Nr=0.1, $\varphi = 0.1$ & Ec=0.1 for various *Bi.*

Figure 10 shows the dimensionless temperature profile of the boundary layer for Alumina-water nanofluid for different volume fraction. It is observed that as volume fraction increases, temperature decreases

The dimensionless temperature profile of the boundary layer for Copper-water nanofluid (Pr = 2.37) and Alumina- water nanofluid (Pr = 6.38) is exhibited in Figure 11. It is noted that as Prandtl number increases, temperature decreases.

In Figure 12, the local heat transfer profiles for Copper- water and Alumina - water nanofluid for different Prandtl numbers are portrayed. It is detected that as Pr increases, local heat transfer profile increases.

In Figure 13, the local heat transfer profiles for Copper- water and Alumina - water nanofluid for

different Radiation parameters are portrayed. It is detected that as Nr increases, local heats transfer profile increases.

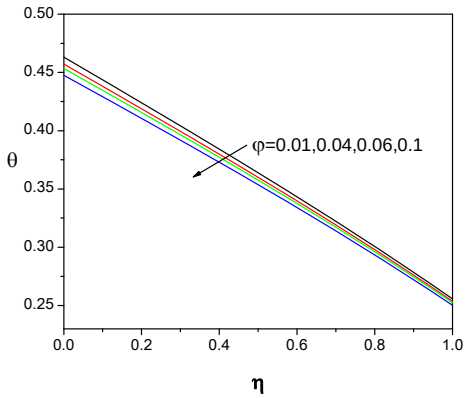

Fig. 10. Effect of volume fraction on temperature profile of alumina water nanofluid.

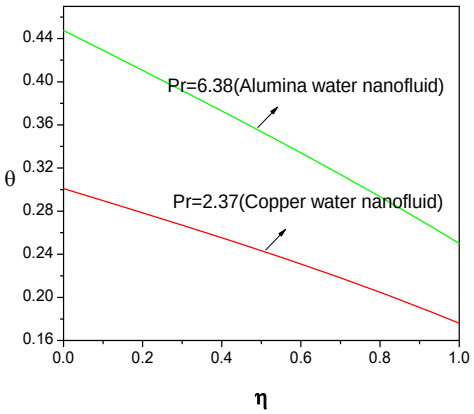

Fig. 11. Temperature profiles of copper water and alumina water nanofluid.

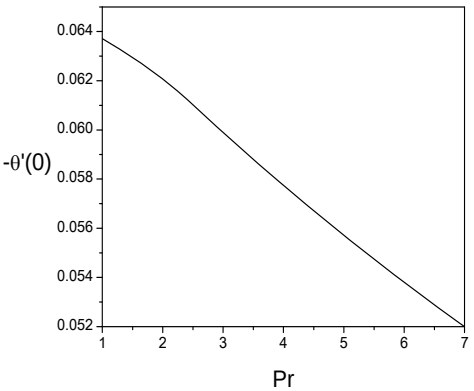

Fig. 12. Local heat transfer varying with different Pr values for Bi=0.1, Nr=0.1, and Ec=0.1.

In Figure 14, the local heat transfer profiles for Copper- water and Alumina - water nanofluid for different Eckert numbers are portrayed and detected that as Ec increases, local heat transfer increases.

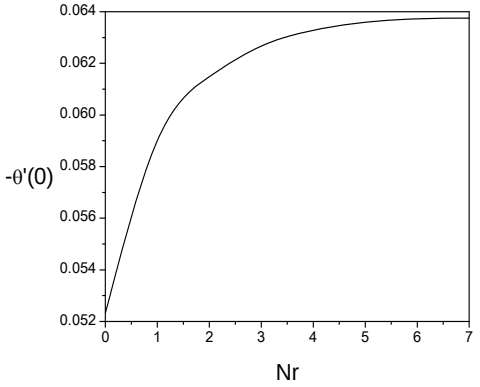

Fig. 13. Local heat transfer varying with different Nr values for Bi=0.1, Ec=0.1, and Pr=6.2.

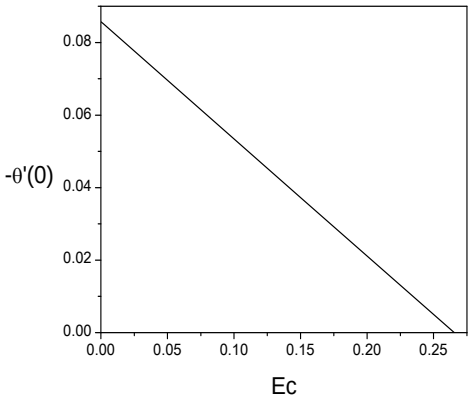

Fig. 14. Local heat transfer varying with different Nr values for Bi=0.1, Ec=0.1, and Pr=6.2.

In Figure 15, the local heat transfer profiles for Copper- water and Alumina - water nanofluid for different Convective heat transfer parameter are portrayed and detected that as Convective heat transfer parameter increases, local heat transfer increases.

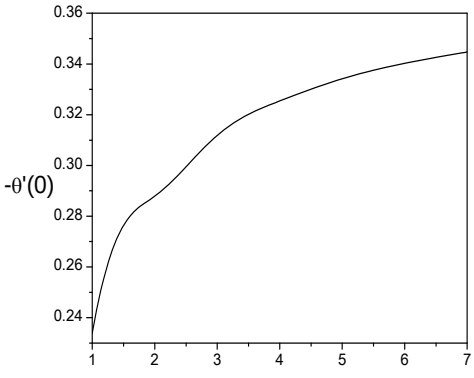

Fig. 15. Local heat transfer varying with different Bi values for Nr=0.1, Ec=0.1, and Pr=6.2.

5. CONCLUSIONS

The present paper investigated the laminar boundary layer flow of copper water and alumina water nanofluids over a vertical plate with radiation and viscous dissipation in the presence of convective boundary condition and suction. The results are presented for various parameters like Prandtl number, volume fraction, Convective heat transfer parameter, Radiation parameter and Eckert number.

- The temperature profiles increase with increase in volume fraction for copper water and alumina water nanofluids.
- The increase in Radiation parameter is to decrease the temperature for both types of nanofluids.
- The increase in Eckert number is to increase the temperature for both types of nanofluids.
- The increase in Prandtl number is to decrease the temperature for both types of nanofluids.
- The increase in Convective heat transfer parameter is to increase the temperature for both types of nanofluids.
- The heat transfer coefficient of nanofluids decreases with the increase of Prandlt number for copper water and alumina water nanofluids.
- The heat transfer coefficient of nanofluids increases with the increase of Radiation parameter for copper water and alumina water nanofluids.
- The heat transfer coefficient of nanofluids decreases with the increase of Eckert number for copper water and alumina water nanofluids.
- The heat transfer coefficient of nanofluids increases with the increase of Convective heat transfer parameter for copper water and alumina water nanofluids.

REFERENCES

Anjali Devi S. P. and A. Julie (2011). Laminar boundary layer flow of nanofluid over a flat plate. *Int. J. of Appl. Math and Mech. 7(6), 52-71.*

Brewster, M. Q. (1992). *Thermal Radiative Transfer Properties.* Wiley, New York.

Christopher, D. M. and B. Wang (2001). Prandtl number effects for Marangoni convection over a flat surface. *International Journal of Thermal Sciences 40, 564-570*.

Emmanuel, C. N. and G. Tushar (2011). Investigations on the nanolayer heat transfer in nanoparticles- in-liquid suspensions. *ARPN Journal of Engineering and Applied Sciences 6, 1.*

Go, J. S., S. J. Kim, G. Lim, H. Yun, J. Lee, I. Song and Y. E. Park (2001). Heat transfer enhancement using flow-induced vibration of a microfin array. *Sens. Actuators A 90, 232–239.*

Golia, C. (1985). Viviani, Marangoni buoyant boundary layers. *L'Aerotechnica Missili e Spazio 64, 29–35.*

Golia, C. and A. Viviani (1986), Non isobaric boundary layers related to Marangoni flows. *Meccanica 21, 200–204.*

Hamad, M. A. A. and I. Pop (2011). Unsteady MHD free convection flow past a vertical permeable flat plate in a rotating frame of reference with constant heat source in a nanofluid Heat Mass Transfer.

Magyari, E. and A. J. Chamkha (2007). Exact analytical solutions for thermosolutal Marangoni convection in the presence of heat and mass generation or consumption. *Heat and Mass Transfer 43, 965-974.*

Maiga, S. E. B., C. T. Nguyen, N. Galanis and G. Roy (2004). Heat transfer behaviors of nanofluids in a uniformly heated tube. *Superlattices and Microstructures 35, 543–557.*

Nor Azizah, Y., A. Ishak, I. Pop and V. Kuppalapalle (2011). Boundary layer flow past a stretching/shrinkingsurface beneath an external uniform shear flowwith a convective surface boundary condition ina nanofluid. *Nanoscale Research Letters 6, 314.*

Sanjeeva, W., C. Haisheng and D. Yulong (2011). Stability of nanofluids in quiescent and shear flow fields. *Nanoscale Research Letters 6, 231.*

Sheikhzadeh, G. A., A. Arefmanesh and M. Mahmoodi (2011). Numerical Study of Natural Convection in a Differentially-Heated Rectangular Cavity Filled with TiO2-Water Nanofluid. *Journal of Nano Research 13, 75-80.*

Tahery, A. A., S. M. Pesteei and A. Zehforoosh (2010). Numerical Study of Heat Transfer Performance of Homogenous Nanofluids under Natural Convection. *International Journal of Chemical Engineering and Applications 1, 1.*

Tania, S. K. and M. A. Samad (2010). Effects of Radiation, Heat Generation and Viscous Dissipation on MHD Free Convection Flow along a Stretching Sheet. *Research Journal of Applied Sciences, Engineering and Technology 2(4), 368-377.*

Tiwari, R. K. and M. K. Das (2007). Heat transfer augmentation in a twosided lid-driven differentially heated square cavity utilizing nanofluids. *Int. J. Heat Mass Transfer 50, 2002–2018.*